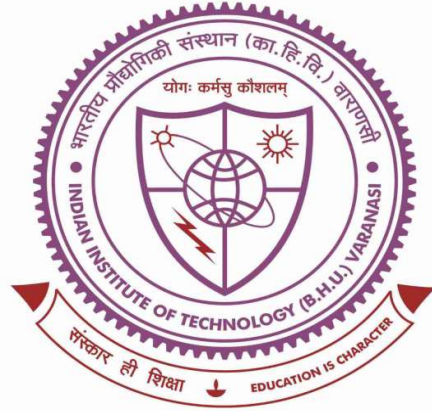


# Impact of Transition Metal Ion Substitution on Physical, Mechanical, Electrical and Biological Characteristics of Bioactive Glasses



A thesis submitted in partial fulfillment for the  
Award of Degree

**DOCTOR OF PHILOSOPHY**

By

***AKANKSHA SINGH***

DEPARTMENT OF CERAMIC ENGINEERING  
INDIAN INSTITUTE OF TECHNOLOGY  
(BANARAS HINDU UNIVERSITY)  
VARANASI – 221005  
INDIA

ROLL No.: 17031002

YEAR: 2024

*Dedicated to my Beloved  
son, husband, Parents  
and Family*

Their blessings and  
prayers accompany me in achieving  
things in my life.



भारतीय  
प्रौद्योगिकी  
संस्थान  
काशी हिन्दू विश्वविद्यालय




INDIAN  
INSTITUTE OF  
TECHNOLOGY  
BANARAS HINDU UNIVERSITY


### CERTIFICATE

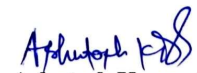
It is certified that the work contained in the thesis titled "*Impact of Transition Metal Ion Substitution on Physical, Mechanical, Electrical and Biological characteristics of Bioactive Glasses*" by "*AKANKSHA SINGH*" has been carried out under my supervision and that this work has not been submitted elsewhere for a degree.

It is further certified that the student has fulfilled all the requirements of the comprehensive examination, candidacy, and SOTA for the award of Ph.D. Degree.

  
**Dr. Preetam Singh**  
Supervisor  
Associate Professor  
Department of Ceramic Engineering  
Indian Institute of Technology (BHU)  
Varanasi - 221005, (U.P.), India

*Dr. Preetam Singh*  
Associate Professor/सह-आचार्य  
Department of Ceramic Engineering  
सैरामिक अभियान्तिकी विभाग  
Indian Institute of Technology (BHU)  
भारतीय प्रौद्योगिकी संस्थान (का०हि०वि०वि०)  
Varanasi-221005/वाराणसी-221005

  
**Prof. Ram Pyare**  
Co-Supervisor  
Professor (Rtd)  
Department of Ceramic Engineering  
Indian Institute of Technology (BHU)  
Varanasi - 221005, (U.P.), India

  
**Dr. Ashutosh Kumar Dubey**  
Head of Department  
Department of Ceramic Engineering  
Indian Institute of Technology (BHU)  
Varanasi - 221005, (U.P.), India

*Dr. Ashutosh Kumar Dubey*  
विभागाध्यक्ष/HEAD  
सैरामिक अभियान्तिकी विभाग  
Department of Ceramic Engineering  
भारतीय प्रौद्योगिकी संस्थान (का०हि०वि०वि०)  
Indian Institute of Technology (B.H.U.)  
Varanasi-221005/वाराणसी-221005



भारतीय  
प्रौद्योगिकी  
संस्थान  
काशी हिन्दू विश्वविद्यालय



INDIAN  
INSTITUTE OF  
TECHNOLOGY  
BANARAS HINDU UNIVERSITY

### DECLARATION BY THE CANDIDATE

I, **Akanksha Singh**, certify that the work embodied in this thesis is my own bonafide work carried out by me under the supervision of **Prof. Ram Pyare and Dr. Preetam Singh** from **July 2017 to June 2024**, at the **Department of Ceramic Engineering**, Indian Institute of Technology (BHU), Varanasi. The matter embodied in this thesis has not been submitted for the award of any other degree/diploma.

I declare that I have faithfully acknowledged and given credits to the research workers wherever their works have been cited in my work in this thesis. I further declare that I have not willfully copied any other's work, paragraphs, text, data, results, *etc.*, reported in journals, books, magazines, reports dissertations, thesis, *etc.*, or available on websites and have not included them in this thesis and have not cited as my own work.

Date: 10.10.2024

Place: IIT (BHU), Varanas

Signature of the student

(Akanksha Singh)

### CERTIFICATE BY THE SUPERVISOR

It is certified that the above statement made by the student is correct to the best of my/our knowledge.

Dr. Preetam Singh 10.10.2024  
Supervisor  
Associate Professor  
Department of Ceramic Engineering  
Indian Institute of Technology (BHU)  
Varanasi - 221005, (U.P.), India  
Associate Professor  
Department of Ceramic Engineering  
सैरामिक अभियान्त्रिकी विभाग  
Indian Institute of Technology (BHU)  
भारतीय प्रौद्योगिकी संस्थान (काशी हिन्दू विश्वविद्यालय)  
Varanasi-221005/वाराणसी-221005

Prof. Ram Pyare  
Co-Supervisor  
Professor (Rtd)  
Department of Ceramic Engineering  
Indian Institute of Technology (BHU)  
Varanasi - 221005, (U.P.), India



भारतीय  
प्रौद्योगिकी  
संस्थान  
काशी हिन्दू विश्वविद्यालय



INDIAN  
INSTITUTE OF  
TECHNOLOGY  
BANARAS HINDU UNIVERSITY

---

**COPYRIGHT TRANSFER CERTIFICATE**

**Title of the Thesis:** *“Impact of Transition Metal Ion Substitution on Physical, Mechanical, Electrical and Biological Characteristics of Bioactive Glasses”*

**Name of the Student:** *Akanksha Singh*

**Copyright Transfer**

**The undersigned hereby assigns to the Indian Institute of Technology (Banaras Hindu University), Varanasi all rights under copyright that may exist in and for the above thesis submitted for the award of the “DOCTOR OF PHILOSOPHY”.**

**Date:** 10.10.2024  
**Place:** IIT (BHU), Varanasi

*Akanksha Singh*  
Signature of the Student  
(Akanksha Singh)

**Note:** However, the author may reproduce or authorize others to reproduce material extracted verbatim from the thesis or derivative of the thesis for the author's personal use provided that the source and the Institute's copyright notice are indicated.

## **Acknowledgments**

The journey toward Ph.D. has been a turning point in my life, and it would not be possible without the constant support, assistance, and guidance that I have received from countless people. I would like to take this opportunity to acknowledge and appreciate those people who have given their valuable time during my Ph.D.

I am thankful to my thesis Supervisor Dr. Preetam Singh, for his constant monitoring, passionate encouragement, continuous instructions, and support in my Ph.D. journey. It would not have been possible to complete my work without his support. Thank you Sir for guiding me.

I am grateful to Co-Supervisor Prof. Ram Pyare, for his persistent monitoring, enthusiastic encouragement, ongoing supervision, and unconditional support throughout my PhD journey. I have always admired his topic expertise, innovative thinking, and passionate approach to study. His creative approach to study inspires me, and it is mirrored in his basic yet simple writing style, which I want to follow in my work. I have been fortunate enough to be part of his group. His suggestions and advice will always be beneficial in life, whether it is academic or non-academic. I am very thankful to you sir for being a mentor academically as well as philosophically and wish to continue to seek this mentorship in future life too.

I am also thankful to my RPEC members, Prof. Santosh Kumar (Mechanical Engineering, IIT-BHU), Dr. and Dr. Anil Kumar for their knowledgeable, motivational, and umpteen suggestions throughout this research work.

I want to express my gratitude to the Head of Department, Ashutosh Kumar Dubey and Ex-Head of Department Vinay Kumar Singh, for providing me required facilities of the

department. I also wish to thank all the faculty members of the Department of Ceramic Engineering, Prof. D. Kumar, Prof. Om Prakash, Prof. S.P. Singh, Prof. Ram Pyare, Prof. Vinay Kumar Singh, Dr. Preetam Singh, Dr. Anil Kumar, Dr. M. R. Majhi, Dr. P. K. Roy, Dr. Ashutosh Dubey, Dr. Santanu Das, Dr. Imteyaz Ahmed, Dr. Sudama Singh, Dr. R.K. Chaturvedi, Dr. Subrata Panda, Dr. Kundan Kumar, Dr. Kaushik Sarkar, Dr. Pawan Pujar, Dr. Akanksha Dwivedi and Dr. Kalyani Mohanta for their motivation, selfless support, and suggestions during course work as well as my whole Ph.D. time.

I would also like to thank Prof. Rajiv Prakash for providing experimental facilities during the entire course of research work at CIFC, IIT (BHU). Along with that, I am also thankful to all the staff at CIFC, IIT (BHU) for their help.

I also gratefully acknowledge the financial support of the Ministry of Education, India (formally known as the Ministry of Human Resource and Development; MHRD, India).

I am also thankful to all non-teaching staff, Mr. Shailendra, Mr. Pawan, Mr. Prasant, Mr. K. K. Maurya, (office staff) Mr. Ashish Tripathi, Mr. Bhagmalji, Mr. Mansa Ram (all Technical and workshop staff) of the Department of Ceramic Engineering for their kind cooperation. I am very thankful to the labmates Dr. V. K. Vyas, Dr. Md. Ershad, Dr. Sushma Yadav, Dr. Dheeraj Kumar and Satendra Kumar Singh for cooperating and maintaining the lab culture. I wish to express my sincere gratitude to all those who have extended their helping hands in various ways during my tenure at the Indian Institute of Technology (Banaras Hindu University), Varanasi, India. I am also thankful for the negative energies that teach me life lessons and help me to grow.

I am highly obliged to my father-in-law Shri Gopal Singh, my parents Shri Rajesh Kumar Singh, Shrimati Madhusheela Singh, my husband Raj Singh, my uncle, my aunty, my younger brothers and sisters and my beloved son Rakshit for their continuous support, love, laughter, and motivation to keep me coherent and to make this project possible,

especially during many rough patches of time. I would like to mention my friends Neeraj, Asim, Anurag, Abhishek, Vaibhav, Pankaj, etc for having that emotional and motivational support during the tenure. Lastly, I want to thank almighty God for all the positive opportunities and negative situations that prepare me to handle situations in the future life.

## LIST OF FIGURES

---

| Figure No.         | Figure description   | Page No. |
|--------------------|--|----------|
| <b>Figure 1.1</b>  | Types of Biomaterial showing their application.  | 4        |
| <b>Figure 1.2</b>  | L.L Hench with 45S5 Bioglass   | 4        |
| <b>Figure 1.3</b>  | Shows the in vitro and in vivo performance of Bone   | 7        |
| <b>Figure 1.4</b>  | Commercially produced glass available in market  | 8        |
| <b>Figure 1.5</b>  | Progression of applications of biomaterials with the corresponding years.  | 8        |
| <b>Figure 1.6</b>  | Chronological analysis of the applications of bioglass in worldwide  | 8        |
| <b>Figure 1.7</b>  | Pictorial representation of bioactive materials surgical implant uses in different human body parts  | 16       |
| <b>Figure 1.8</b>  | Bioactive regions in the CaO-SiO <sub>2</sub> -Na <sub>2</sub> O system  | 17       |
| <b>Figure 1.9</b>  | Schematic illustration of the dissolving behaviour of silicate and borate bioactive glasses in simulated bodily fluid (Henao et al. 2019). | 23       |
| <b>Figure 1.10</b> | Schematic representation of the formation of hydroxy carbonate apatite (HCA) on the surface of bioactive glasses.                          | 23       |
| <b>Figure 1.11</b> | Chemical composition of Borosilicate Glass   | 24       |
| <b>Figure 1.12</b> | Comparison between crystalline and non-crystalline (amorphous) silica structure  | 25       |
| <b>Figure 1.13</b> | (a) Tetrahedral structural unit of silica (SiO <sub>2</sub> ). (b) Effect of introduction of Na <sup>+</sup> cations in a silica network   | 27       |
| <b>Figure 2.1</b>  | Globar Furnace used for melting  | 39       |
| <b>Figure 2.2</b>  | Steps for Solid-State Technique and further characterization.  | 40       |
| <b>Figure 2.3</b>  | (a) Glass Melting (b) Melted glass samples casted in steel mould   | 43       |
| <b>Figure 2.4</b>  | Schematic diagram for preparation of pallets through Solid-State Synthesis route.  | 44       |
| <b>Figure 2.5</b>  | Schematic representation of the reaction upon body fluids contact  | 45       |

|                     |   |    |
|---------------------|---|----|
| <b>Figure 2.6</b>   | Density measurement instrument [Sartorius BSA2245CW] (a) Density kit and (b) Electric Weighing Balance  | 46 |
| <b>Figure 2.7</b>   | Microprocessor based pH meter   | 46 |
| <b>Figure 2.8</b>   | Olympus instrument (M-45, USA)  | 48 |
| <b>Figure 2.9</b>   | DSC/TGA Instrument  | 49 |
| <b>Figure 2.10</b>  | Schematic representations Dielectric Test station   | 51 |
| <b>Figure 2.11</b>  | Demonstration for Bragg's Law   | 53 |
| <b>Figure 2.12</b>  | Principle of XRD  | 54 |
| <b>Figure 2.13</b>  | X-Ray Diffractometer Instrument   | 54 |
| <b>Figure 2.14</b>  | FTIR Spectrometer Instrument  | 56 |
| <b>Figure 2.15</b>  | Principle of FTIR   | 57 |
| <b>Figure 2.16</b>  | Working OF FTIR   | 58 |
| <b>Figure 2.17</b>  | SEM/EDS Instrument  | 59 |
| <b>Figure 2.18</b>  | Schematic diagram of SEM  | 60 |
| <b>Figure 2.19</b>  | Bio-rad iMark™ microplate absorbance reader for cellular analysis   | 61 |
| <b>Figure 2.20</b>  | Inverted fluorescence phase contrast microscope   | 63 |
| <b>Figure 3.1</b>   | pH value variation after immersion in SBF for base and different V <sub>2</sub> O <sub>5</sub> substituted borosilicate glass.  | 77 |
| <b>Figure 3.2</b>   | XRD graph for base and V <sub>2</sub> O <sub>5</sub> substituted borosilicate samples (a) before and (b) after immersion in SBF solution  | 79 |
| <b>Figure 3.3</b>   | FTIR graph for base and V <sub>2</sub> O <sub>5</sub> substituted borosilicate samples (a) before and (b) after 28 days of immersion in SBF   | 80 |
| <b>Figure 3.4.1</b> | SEM/EDX image of base borosilicate glass samples (a) SEM image before SBF immersion (b) SEM image after 28 days immersion in SBF solution (c) EDX image after SBF immersion in SBF solution                                     | 81 |
| <b>Figure 3.4.2</b> | SEM/EDX image of 0.1% V <sub>2</sub> O <sub>5</sub> doped borosilicate glass samples (a) SEM image before SBF immersion (b) SEM image after 28 days immersion in SBF solution (c) EDX image after SBF immersion in SBF solution | 82 |
| <b>Figure 3.4.3</b> | SEM/EDX image of 0.3% V <sub>2</sub> O <sub>5</sub> doped borosilicate glass samples  | 82 |

|                     |  |    |
|---------------------|--|----|
|                     | (a) SEM image before SBF immersion (b) SEM image after 28 days immersion in SBF solution (c) EDX image after SBF immersion in SBF solution   |    |
| <b>Figure 3.4.4</b> | SEM/EDX image of 0.5% V <sub>2</sub> O <sub>5</sub> doped borosilicate glass samples (a) SEM image before SBF immersion (b) SEM image after 28 days immersion in SBF solution (c) EDX image after SBF immersion in SBF solution  | 82 |
| <b>Figure 3.4.5</b> | SEM/EDX image of 1% V <sub>2</sub> O <sub>5</sub> doped borosilicate glass samples (a) SEM image before SBF immersion (b) SEM image after 28 days immersion in SBF solution (c) EDX image after SBF immersion in SBF solution  | 83 |
| <b>Figure 3.4.6</b> | SEM/EDX image of 2.5% V <sub>2</sub> O <sub>5</sub> doped borosilicate glass samples (a) SEM image before SBF immersion (b) SEM image after 28 days immersion in SBF solution (c) EDX image after SBF immersion in SBF solution  | 83 |
| <b>Figure 3.4.7</b> | SEM/EDX image of 4% V <sub>2</sub> O <sub>5</sub> doped borosilicate glass samples (a) SEM image before SBF immersion (b) SEM image after 28 days immersion in SBF solution (c) EDX image after SBF immersion in SBF solution  | 83 |
| <b>Figure 3.5</b>   | Ex vivo Hemocompatibility of the developed product; (A) represents the after haemolytic study, (B) % of haemolytic activity of different base and V <sub>2</sub> O <sub>5</sub> substituted borosilicate samples   | 84 |
| <b>Figure 3.6.1</b> | Cytotoxic investigations of V <sub>2</sub> O <sub>5</sub> substituted borosilicate glass samples (Base, 0.1%, 0.3%, 0.5%, 2.5% and 4%) against MG-63 cell line   | 86 |
| <b>Figure 3.6.2</b> | Phase contrast microscopic images of V <sub>2</sub> O <sub>5</sub> substituted borosilicate glass samples (Base, 0.1%, 0.3%, 0.5%, 2.5% and 4%) against MG-63 cell line at different concentration showing proliferation of cells in concentration dependent manner except in 2.5% and 4%. | 86 |
| <b>Figure 3.7</b>   | Dependence of permittivity vs frequency for base and 2.5% V <sub>2</sub> O <sub>5</sub> substituted Borosilicate glass (a) before and (b) after immersion in SBF for 28 days   | 88 |
| <b>Figure 3.8</b>   | Dependence of Dielectric loss with respect to frequency of base and  | 88 |

|                     |   |     |
|---------------------|---|-----|
|                     | 2.5% V <sub>2</sub> O <sub>5</sub> substituted borosilicate glass (a) before and (b) after immersion in SBF for 28 days   |     |
| <b>Figure 4.1</b>   | pH variation of prepared samples  | 99  |
| <b>Figure 4.2</b>   | FTIR graph for (a) Vb1 (b) Vb2 (c) Vb3 (d) Vb4 samples for corresponding SBF immersion days   | 100 |
| <b>Figure 4.3</b>   | XRD graph for V <sub>2</sub> O <sub>5</sub> substituted 1393-B3 glass (a) before SBF and after SBF immersion for (b) 15 days (c) 28 days, SBF images for the samples (d) before SBF and SBF immersion for (e)15 days (f)28 days     | 101 |
| <b>Figure 4.4</b>   | Ex vivo Hemocompatibility and cellular compatibility of the developed product; (a) represents the after haemolytic study, (b) % of haemolytic activity (c) % Cellular viability (d) Phase contrast image for variable concentration | 102 |
| <b>Figure 5.1</b>   | (a) pH value (b) Density of base, and TiO <sub>2</sub> substituted 1393-B3 glass samples  | 115 |
| <b>Figure 5.2</b>   | Mechanical properties variation of base and TiO <sub>2</sub> substituted 1393-B3 glass samples (a) Compressive strength and (b) Flexural strength   | 116 |
| <b>Figure 5.3</b>   | DSC graph of base 1393-B3 borate glass before sintering   | 118 |
| <b>Figure 5.4</b>   | Thermal properties of base and TiO <sub>2</sub> substituted 1393-B3 glass samples (a) DSC graph and (b) TGA graph   | 119 |
| <b>Figure 5.5</b>   | FTIR spectrum for different compositions of TiO <sub>2</sub> substituted 1393-B3 borate glass before immersion in SBF.  | 120 |
| <b>Figure 5.6</b>   | FTIR spectrum for BG1(1%), BG2(1.5%), BG3(2%) and BG4(2.5%) for different TiO <sub>2</sub> substituted 1393-B3 borate glass after 1,7,15,21 and 28 days immersion in SBF solution   | 120 |
| <b>Figure 5.7</b>   | XRD graph of different wt % of TiO <sub>2</sub> substitution in 1393-B3 borate glass (a) before SBF immersion and (b) after SBF immersion   | 121 |
| <b>Figure 5.8.1</b> | SEM image for base 1393-B3 borate bioactive glass sample (a) before SBF immersion and (b) after SBF immersion   | 122 |
| <b>Figure 5.8.2</b> | SEM-EDS image for 1 % TiO <sub>2</sub> substituted 1393-B3 borate bioactive glass sample (a) before SBF immersion and (b) after SBF immersion.  | 122 |

|                      |  |     |
|----------------------|--|-----|
| <b>Figure 5.8.3</b>  | SEM-EDS image for 1.5 % TiO <sub>2</sub> substituted 1393-B3 borate bioactive glass sample (a) before SBF immersion and (b) after SBF immersion  | 123 |
| <b>Figure 5.8.4</b>  | SEM-EDS image for 2 % TiO <sub>2</sub> substituted 1393-B3 borate bioactive glass sample (a) before SBF immersion and (b) after SBF immersion  | 123 |
| <b>Figure 5.8.5</b>  | SEM-EDS image for 2.5 % TiO <sub>2</sub> substituted 1393-B3 borate bioactive glass sample (a) before SBF immersion and (b) after SBF immersion  | 124 |
| <b>Figure 5.9</b>    | Ex vivo haemocompatibility of the TiO <sub>2</sub> substituted 1393-B3 borate glass (A) represents the after haemolytic study, (B) % of haemolytic activity  | 125 |
| <b>Figure 5.10.1</b> | Bar diagram represents a cellular proliferation of titanium substituted with 1393-B3 borate glass sample against MG-63 cell line. Here * denotes a significant difference (p<0.05) compared to the control.  | 125 |
| <b>Figure 5.10.2</b> | Phase contrast microscopic images (400µm) of TiO <sub>2</sub> substituted 1393-B3 glass samples (Base, 1%, 1.5%, 2%, and 2.5%) against MG-63 cell lines at various concentrations (100, 200,400 and 600µg/ml) showing proliferation of cells in a concentration-dependent manner | 126 |
| <b>Figure 6.1</b>    | (a) Variation of density with increasing content of ZrO <sub>2</sub> in 1393-B3 Borate glass(b) The pH value of SBF varies with the amount of days that BZ samples are submerged in it   | 143 |
| <b>Figure 6.2.1</b>  | DSC/TGA analysis of base 1393-B3 borate glass  | 144 |
| <b>Figure 6.2.2</b>  | (a) DSC and (b)TGA graph of base and different wt% of ZrO <sub>2</sub> substitution in 1393-B3 borate glass  | 144 |
| <b>Figure 6.3</b>    | Mechanical properties variation of base and ZrO <sub>2</sub> substituted 1393-B3 glass samples (a) Compressive strength and (b) Flexural strength  | 145 |
| <b>Figure 6.4.1</b>  | FTIR spectrum for different compositions of ZrO <sub>2</sub> substituted 1393-B3 borate glass before immersion in SBF  | 146 |

|                     |   |     |
|---------------------|---|-----|
| <b>Figure 6.4.2</b> | FTIR spectrum for BZ1(1%), BZ2(1.5%), BZ3(2%) and BZ4(2.5%) for different ZrO <sub>2</sub> substituted 1393-B3 borate glass after 1,7,15,21 and 28 days immersion in SBF solution.  | 147 |
| <b>Figure 6.5.1</b> | XRD graph of different wt % of ZrO <sub>2</sub> substitution in 1393-B3 borate glass (a) before SBF immersion and (b) after SBF immersion   | 148 |
| <b>Figure 6.5.2</b> | XRD graph of different 1.5 wt % of ZrO <sub>2</sub> (BZ2) substitution in 1393-B3 borate glass (a) before SBF immersion and (b) after SBF immersion   | 149 |
| <b>Figure 6.6.1</b> | SEM image for Base 1393-B3 borate bioactive glass sample (a) SEM before SBF immersion (b) SEM after 28 days SBF immersion (c) EDS spectrum after 28 days SBF immersion  | 150 |
| <b>Figure 6.6.2</b> | SEM images for 1 wt% ZrO <sub>2</sub> substituted 1393-B3 borate bioactive glass sample (a) before SBF immersion (b) after 28 days SBF immersion and for 1.5 wt% ZrO <sub>2</sub> substituted 1393-B3 borate bioactive glass sample (c) before SBF immersion (d) after 28 days SBF immersion            | 150 |
| <b>Figure 6.6.3</b> | SEM images for 2 wt% ZrO <sub>2</sub> substituted 1393-B3 borate bioactive glass sample (a) before SBF immersion (b) after 28 days SBF immersion and SEM images for 2.5 wt% ZrO <sub>2</sub> substituted 1393-B3 borate bioactive glass sample (c) before SBF immersion (d) after 28 days SBF immersion | 151 |
| <b>Figure 6.6.4</b> | EDS spectrum image after 28 days SBF immersion for (a) 1.5 wt% ZrO <sub>2</sub> (b) 2.5 wt% ZrO <sub>2</sub> substituted 1393-B3 borate bioactive glass sample after SBF immersion  | 151 |
| <b>Figure 6.7</b>   | Ex vivo hemocompatibility of different wt% of ZrO <sub>2</sub> substituted 1393-B3 borate glass (a) represents the after haemolytic study, (b) % of hemolytic activity  | 152 |
| <b>Figure 6.8.1</b> | Bar diagram represents a cellular proliferation of titanium substituted with 1393-B3 borate glass sample against MG-63 cell line. Here * denotes a significant difference (p<0.05) compared to the control  | 153 |
| <b>Figure 6.8.2</b> | Phase contrast microscopic images (400µm) of ZrO <sub>2</sub> substituted 1393-B3 glass samples (Base, 1%, 1.5%, 2%, and 2.5%) against  | 153 |

MG-63 cell lines at various concentrations (100, 200,400 and 600µg/ml) showing proliferation of cells in a concentration-dependent manner

|                     |  |     |
|---------------------|--|-----|
| <b>Figure 7.1</b>   | (a) Illustration of Electro thermal poling Experiment (b) After poling, the negative and positive charged surfaces are designated as “N-Surface” and “P-Surface”   | 168 |
| <b>Figure 7.2</b>   | (a) DTA value (b) Density of base, and ZnO substituted 45S5 bioglass samples   | 169 |
| <b>Figure 7.3</b>   | FTIR of ZnO substituted 45S5 bioglass (a) before immersion in SBF (b) after 15 days of immersion in SBF solution   | 169 |
| <b>Figure 7.4.1</b> | XRD of (a) base and ZnO substituted 45S5 bioglass before immersion in SBF (b) unpoled and poled N and P surface after 15 days of immersion in SBF solution.  | 171 |
| <b>Figure 7.4.2</b> | XRD pattern of (a) ZnO substituted 45S5 bioglass Unpoled samples (b) Negative charged sample with different concentration after immersion in SBF for 15 days   | 171 |
| <b>Figure 7.5</b>   | SEM images analysis of (a) base samples (b) 1% mole concentration ZnO substituted samples and (c) 3% mole concentration ZnO substituted samples after SBF immersion for unpoled sample, ‘N’ Surface of polarized sample and ‘P’ Surface of polarized sample respectively | 172 |
| <b>Figure 7.6</b>   | EDS analysis of (a) Calcium mole concentration (b) EDS analysis of Phosphorous mole concentration  | 173 |
| <b>Figure 7.7</b>   | AFM analysis of Base sample’s surface after SBF immersion (a) unpoled sample (b) ‘N’ Surface of polarized sample   | 174 |
| <b>Figure 7.8</b>   | AFM analysis of analysis of Zn (1% mole) concentration sample after SBF immersion (a) unpoled sample (b) ‘N’ Surface of polarized sample   | 174 |
| <b>Figure 7.9</b>   | AFM analysis of analysis of Zn (5% mole) concentration sample after SBF immersion (a) unpoled sample (b) ‘N’ Surface of polarized sample   | 175 |
| <b>Figure 7.10</b>  | AFM results obtained for the samples are displayed in the bar graph  | 175 |

**Figure 7.11** (a) Real part of Relative permittivity (b) A.C. Conductivity versus Frequency 176

---

## LIST OF TABLES

---

| Table No.        | Table description   | Page No. |
|------------------|---|----------|
| <b>Table 1.1</b> | Numerous factors to consider while selecting materials for biomedical applications                          | 12       |
| <b>Table 1.2</b> | Ion Concentration (mM/L) of simulated body fluid (SBF) and human blood plasma                               | 13       |
| <b>Table 1.3</b> | The application of silica-based bioactive glasses in medical facilities                                     | 15       |
| <b>Table 2.1</b> | Weight % composition of V <sub>2</sub> O <sub>5</sub> substituted borosilicate glass                        | 41       |
| <b>Table 2.2</b> | Weight % composition of V <sub>2</sub> O <sub>5</sub> substituted 1393-B3 Boarte glass                      | 41       |
| <b>Table 2.3</b> | Weight % composition of TiO <sub>2</sub> substituted 1393-B3 Boarte glass                                   | 41       |
| <b>Table 2.4</b> | Weight % composition of ZrO <sub>2</sub> substituted 1393-B3 Boarte glass                                   | 42       |
| <b>Table 2.5</b> | Mole % composition of ZnO substituted 45S5 glass  | 42       |
| <b>Table 2.6</b> | Chemicals used for the preparation of simulated body fluid (SBF)  | 53       |
| <b>Table 3.1</b> | Weight % composition of V <sub>2</sub> O <sub>5</sub> substituted borosilicate glass                        | 71       |
| <b>Table 3.2</b> | Chemical composition, molar volume, density and compressive strength of glass samples:                      | 77       |
| <b>Table 4.1</b> | Bioactive V <sub>2</sub> O <sub>5</sub> substituted 1393-B3 glass compositions (wt %)                       | 97       |
| <b>Table 5.1</b> | Composition of BG bioactive glass (wt%)   | 110      |
| <b>Table 5.2</b> | Longitudinal velocity and transverse velocity   | 117      |
| <b>Table 5.3</b> | Poisson's ratio, young's modulus, bulk modulus and shear modulus values                                     | 117      |
| <b>Table 6.1</b> | Chemical composition of the BZ sample (wt %)  | 138      |
| <b>Table 7.1</b> | Mole % composition of ZBG bioactive glass samples   | 165      |
| <b>Table 7.2</b> | Absorbance Intensity Ratio of P-O Bending at 560 cm <sup>-1</sup> over Si-O Bending at 470 cm <sup>-1</sup> | 170      |

|                  |   |     |
|------------------|---|-----|
| <b>Table 7.3</b> | Dielectric constant value of corresponding samples at 1 KHz frequency | 177 |
| <b>Table 8.1</b> | Comparative analysis of properties of all the synthesized materials   | 188 |

## **LIST OF ABBREVIATIONS**

---

| <b>Notation</b> | <b>Abbreviations</b>                            |
|-----------------|---|
| <i>et al.</i>   | et alia, Latin for “and others “                |
| <i>i.e.</i>     | That is   |
| <i>e.g.</i>     | Example   |
| <i>etc.</i>     | Et cetera, Latin for “and other similar things” |
| BG              | Bioactive Glass                                 |
| <i>viz.</i>     | Namely  |
| Mg              | Milligram                                       |
| G               | Gram  |
| Cm              | Centimeter                                      |
| Hz              | Hertz   |
| Min             | Minute  |
| Hr              | Hour  |
| s <sup>-1</sup> | Per Second                                      |
| IR              | Infrared  |
| BG              | Bioactive Glass                                 |
| BGs             | Bioactive glass derivatives                     |
| XRD             | X-ray diffractometer                            |
| SEM             | Scanning electron microscopy                    |
| FTIR            | Fourier Transform Infrared spectroscopy         |
| EDS             | Energy dispersive X-ray spectroscopy            |
| SBF             | Simulated Body Fluid                            |
| PBS             | Phosphate-buffered saline                       |
| RBCs            | Red Blood Cells                                 |
| OD              | Optical Density                                 |
| RT or rt        | Room temperature                                |
| MHz             | Megahertz                                       |
| PVA             | Polyvinyl Alcohol                               |
| HA, Hap         | Hydroxyapatite                                  |
| HCA             | Hydroxycarbonate apatite                        |
| MG-63           | Human osteosarcoma cell line                    |
| DMEM            | Dulbecco's Modified Eagle Medium                |
| FBS             | Fetal bovine serum                              |
| E               | Applied Electric field                          |
| AFM             | Atomic force microscopy                         |
| Tris<br>buffer  | Tris-hydroxymethyl aminomethane                 |

|       |                         |
|-------|-------------------------|
| $T_c$ | Curie temperature       |
| J     | Leakage current density |
| P     | Polarization vector     |
| T     | Temperature             |
| R     | Resistance              |
| C     | Capacitance             |
| K     | Kilo                    |

| <b>Symbols used</b> |                         |
|---------------------|-------------------------|
| <b>Symbols</b>      | <b>Full name</b>        |
| K                   | Kelvin                  |
| °C                  | Degree Celsius          |
| $\sigma$            | Conductivity            |
| $\chi^2$            | Chi square              |
| $\delta$            | Delta                   |
| >                   | Greater than            |
| <                   | Less than               |
| $\Lambda$           | Wavelength              |
| $\Omega$            | Omega                   |
| E                   | Dielectric permittivity |

## **PREFACE**

This thesis describes the synthesis of transition metal ions like vanadium, titanium, zirconium and zinc ions substitution to bioactive glasses. Melt-quench technique was used to synthesize vanadium-substituted borosilicate glass, zirconium, vanadium, and titanium-substituted 1393-B3 borate glass and zinc substituted 45S5 glass. Characterization was achieved by both in vitro and in vivo experiments. Mechanical properties of the therapeutic ions-derived glass samples, along with parent glass-based glass samples, were examined by measuring the compressive strength, flexural strength and modulus of elasticity. Archimedes' principle analyzes physical property such as density. The characterization process includes in vitro bioactivity and cytocompatibility, hemocompatibility, as well as electrical performance. In vitro bioactivity was assessed using structural (XRD), functional (FTIR), and morphological (SEM-EDS) alterations caused by surface modification, as well as chemical behavioural (pH) changes induced by ion exchange in SBF (simulated bodily fluid). The hemocompatibility of materials is investigated using human blood red blood cells. The in vitro cytocompatibility of glass samples was investigated using MG-63 (Human osteosarcoma cell) to determine cellular viability, growth, and cytotoxicity. Bioactive glasses have medicinal applications in orthopaedic implants.

**Chapter 1** presents the introduction of biomaterials and their application to modern medical techniques and a way forward to develop superior bioactive materials for different human body implants in case bone fractures and severe diseases.

**Chapter 2** deals with synthesis and characterization techniques utilized in physico-chemical, mechanical, electrical properties, *in-vitro* study, hemocompatibility and the study of the MG-63 cell line growth to check the cellular compatibility of the materials.

**Chapter 3** presents the investigation of bioactivity of borosilicate glass samples with the substitution of  $V_2O_5$  (0-4 wt%). In-vitro bioactivity studied by FTIR, XRD, and SEM/EDS technique after SBF immersion. Physico-chemical, mechanical and electrical properties have been

studied. The results are studied considering the formation of HA layer on the glass surface. Hemocompatibility was tested with human blood, and cellular compatibility were performed on the MG-63 cell line.

**Chapter 4** presents the investigation of bioactivity of 1393-B3 borate glass samples with the substitution of  $V_2O_5$  (0-2.5 wt%). In-vitro bioactivity of the samples studied with FTIR, XRD, and SEM/EDS technique after SBF immersion. Hemocompatibility was assessed using human blood, while cellular compatibility was done using the MG-63 cell line.

**Chapter 5** presents the investigation of bioactivity of 1393-B3 borate glass samples with the substitution of  $TiO_2$  (0-2.5 wt%). Physical, mechanical and thermal properties were determined. The in-vitro bioactivity of the samples was examined using FTIR, XRD, and SEM/EDS techniques after SBF immersion. Hemocompatibility was determined using human blood, while cellular compatibility was determined using the MG-63 cell line.

**Chapter 6** presents the investigation of bioactivity of 1393-B3 borate glass samples substituted with  $ZrO_2$ (0-2.5 wt%). Physical, mechanical and thermal properties are studied. After immersing the samples in SBF, in-vitro bioactivity was investigated using FTIR, XRD, and SEM/EDS techniques. Hemocompatibility and cellular compatibility were determined.

**Chapter 7** presents the investigation of bioactivity of ZnO (0-3 mole %) substituted 45S5 glass before and after polarization process. In-vitro studied with the help of FTIR, XRD, SEM/EDS, and AFM techniques to find HA layer. Electrical properties of the samples were studied.

**Chapter 8** provides the conclusion of the entire work. The future scope is also included in this chapter which is the proposal based on the results and explanation obtained in this thesis work.